JOURNAL OF MATERIALS SCIENCE **36** (2001) 4433–4441

# On the meaning of the impingement parameter in kinetic equations for nucleation and growth reactions

M. J. STARINK
*Materials Research Group, School of Engineering Sciences, University of Southampton, Southampton S017 1BJ, UK*
*E-mail: M.J.Starink@soton.ac.uk*

If certain preconditions are met, the Johnson-Mehl-Avrami-Kolmogorov (JMAK) kinetic equation is exactly accurate for nucleation and growth reactions with linear growth and is, at least, a good approximation for nucleation and growth reactions with parabolic growth. These preconditions include randomly distributed product phases, isotropic growth and constant equilibrium state. Mechanisms causing deviations from these preconditions include: capillarity effect, vacancy annihilation, blocking due to anisotropic growth. It is shown that deviations lead to a modification of the overall transformation, which can be approximated well by a single equation:

$$\alpha = 1 - \left[\frac{(k(T)t)^{n_s}}{\eta_i} + 1\right]^{-\eta_i}$$

where $\alpha$ is the fraction transformed, $\eta_i$ is the impingement parameter, $n_s$ and $k(T)$ are parameters that depend on growth geometry and growth rate. The factors which influence the impingement parameter are discussed. 

## 1. Introduction

In studies of nucleation and growth type reactions, often the Johnson-Mehl-Avrami-Kolmogorov (JMAK) equation [1–6] is assumed to be valid. In generalised form the JMAK equation gives the (average) fraction transformed, $\alpha$, as a function of the time, $t$, for isothermal reactions:

$$\alpha = 1 - \exp\lfloor -(k(T)t)^{n_A} \rfloor \quad (1)$$

where $n_A$ is a constant often referred to as the Avrami exponent and $k(T)$ is a temperature dependent factor (often taken as an Arrhenius type expression). The general equation for $n_A$ is [2, 7]:

$$n_A = N_{\dim} g + B \quad (2)$$

where $g$ is 1 for linear growth or 1/2 for parabolic (diffusion controlled) growth, $B$ is 0 in the case of site saturation (no nucleation during the transformation), or 1 for continuous nucleation (at constant nucleation rate), $N_{\dim}$ is the dimensionality of the growth. The JMAK equation (Equation 1) has been applied to many nucleation and growth type reactions, including such diverse reactions as diffusion controlled precipitation (for recent examples see e.g. [8–11]), recrystallisation (e.g. [12]), ferroelectric/ferromagnetic switching (e.g. [13]), surface growth in gas/vacuum environments (e.g. [14]). Materials analysed range from lipids, sugars, polymers, to metals and rock. Notwithstanding the apparent wide range of applicability, many cases of deviations from JMAK kinetics have been reported [7, 15–27]. Understanding the causes of deviations from standard JMAK kinetics and the development of improved models is an important interdisciplinary research area. For example, in metal processing, it is important because JMAK models are used in models for various industrial processes (e.g. in models for precipitation and concomitant precipitation hardening in industrial Al-based alloys [8, 28]).

It is thought that deviations from the JMAK equation can generally be explained by a breakdown of assumptions made in the derivation of the JMAK model, and in the present work, we will investigate the consequences of such deviations from these assumptions. Recently, it has been shown [21–26] that several precipitation reactions which do not fit to JMAK kinetics can be fitted by an equation of the type:

$$\alpha = 1 - \left[\frac{(k(T)t)^{n_S}}{\eta_i} + 1\right]^{-\eta_i} \quad (3)$$

where $\eta_i$ is the so-called impingement parameter, $n_S$ is a parameter akin to the Avrami exponent in Equation 1,

$k(T)$ has the same meaning as in Equation 1. The latter equation was derived by using the extended volume (see e.g. [4, 21, 29]), and impingement is taken into account by using:

$$\frac{d\alpha}{d\alpha_{\text{ext}}} = (1-\alpha)^{\lambda_i} \tag{4}$$

where $\alpha_{\text{ext}}$ is the extended fraction transformed and $\lambda_i$ is a (positive) constant ($\eta_i = 1/(\lambda_i - 1)$).* Equation 3 incorporates the JMAK equation: in the limit for $\eta_i \to \infty$ Equations 1 and 3 are equivalent and $n_A = n_S$ [21]. As detailed in previous work (see e.g. [2, 16, 21, 24, 30–32]), the extended fraction transformed, $\alpha_{\text{ext}}$, is directly related to rate of growth of individual nuclei and the nucleation rate.

It is noted that the above treatment of impingement is not a rigorous statistical treatment. Instead, Equation 4 represents an approximation that uses an impingement parameter which, at this stage, has a very limited physical meaning. The meaning of the impingement parameter, at this stage, can only be defined for limited cases, e.g. for $\lambda_i = 1$ impingement is identical to JMAK impingement, which represent an idealised case, the preconditions of which are detailed in the next section. In previous works [21–27] the use of the adjustable impingement parameter $\eta_i$ was based mainly on a good fit with experimental data, and no theoretical justification was provided. In the present work, it will be shown how Equation 3, and specifically the adjustable impingement parameter $\eta_i$, can be justified. In addition, the physical meaning of $\eta_i$ will be investigated by determining how microstructural and kinetic parameters influence it.

## 2. Theory: breakdown of JMAK assumptions and its consequences

Recent theoretical work [3, 33] has proven that the JMAK kinetic equation is accurate for reactions with linear growth,† provided:

i) the sample is initially homogeneous,
ii) product phases are randomly distributed,
iii) if nucleation occurs, nuclei are randomly distributed,
iv) average growth rates are independent of position in the sample,
v) the reaction is not influenced by any time-dependent process (defect annihilation/creation, relieving/creation of internal stresses) in the sample which is not directly related to the transformation studied,
vi) impingement on objects other than neighbouring domains of the product phase is negligible,
vii) so-called blocking resulting from anisotropic growth (34–37) is negligible, and
viii) the equilibrium state is constant, i.e. the amount that can transform does not depend on time (this assumption can breakdown under non-isothermal conditions, see e.g. [21, 24]).

We will refer to these as JMAK assumptions i–viii. Theoretical investigations into the effect of the breakdown of assumptions ii [38], iii-iv [39], vi [30, 40] and vii [34–37, 41] have been performed: they show that in these cases deviations from the JMAK kinetic equation (Equation 1) occur and that, in general, impingement becomes stronger, which results in a slowing down of the later stages of the reaction.

For parabolic (i.e. diffusion controlled) growth reactions, the impingement of diffusion fields around randomly distributed precipitates (so-called soft impingement) is an extremely complex mathematical problem. The problem is simplified for regular arrays, and Ham [42, 43] has shown that for precipitates growing in 3 dimensions situated on a regular cubic array, JMAK kinetics is accurate up to a transformed fraction of about 0.7 to 0.8, whilst for later stages the reaction is slightly slower than JMAK kinetics. Taking into account that changing from a regular array to a random distribution of growing product phase will generally speed up the latter stages of the transformation, this indicates that also for parabolic growth reactions which conform to the JMAK assumptions, JMAK kinetics is, at least in good approximation, accurate. Also Monte Carlo simulations of the transformations of grains which grow according to a diffusion controlled mechanism (i.e. growth rate is proportional to the inverse of the particle radius) indicate that JMAK kinetics is, at least, a good approximation for diffusion controlled transformations [44]. A similar conclusion was reached by Uebele and Hermann [38] who approximated diffusion controlled growth in a mathematical model which considers parabolic growth and hard impingement. Their work shows that although strictly speaking the Equation 1 is not valid, deviations from this equation are very small and may in practice be neglected. From these works we may conclude that Equation 1 is at least a very good approximation of the transformed fraction in a diffusion controlled reaction. As it will be shown in this paper that for precipitation reactions the JMAK assumptions are generally not valid, the discussion on whether JMAK kinetics is exact or just an accurate approximation, will not be further pursued.

Deviations from assumptions i–viii will result in a modification of the overall kinetics of the reaction. In this section, several of these deviations will be considered and it will be shown how they (may) influence the overall kinetics.

### 2.1. Inhomogeneous sample

If the sample is inhomogeneous, the amount of product phase may vary with position in the sample. Consider

* Different authors have used different definitions and/or symbols $(c, i, \gamma)$ to express the degree of impingement within the same framework that forms the basis for Equations 3 and 4. To convert between the expressions used in this work and Refs. [15, 21–27, 29, 30] use $\lambda_i = c + 1 = i = 2 - \gamma$. Note also that in several works different symbols for the fraction transformed are used, whilst the meaning of $k$ differs somewhat between the different publications.

† Note that this proof shows that the treatment proposed in Refs. [16, 17] in which the so-called phantom nuclei are eliminated, is incorrect. Hence, this treatment cannot form the basis for an explanation of deviations from the JMAK theory (see also [4, 5, 6]).

for example a sample in which the concentration of reactant is different in different areas of the sample, whilst all areas transform according to JMAK kinetics with the same $k$ and $n$ to a product phase. Clearly the average concentration transformed on completion of the reaction is the average concentration of reactant available and it is readily verified that the overall kinetics of transformation conform to JMAK kinetics (Equation 1). Hence, for an inhomogeneous sample with constant $k$ and $n$ the overall transformation equation is unchanged: if individual areas transform according to JMAK kinetics also the average over the whole sample will conform to JMAK kinetics.

## 2.2. Nucleation and growth rates that vary with position

In contrast to the previous case, variation in the growth rate will alter the overall kinetic equation for the reaction. To illustrate this, we first consider a general case in which $k$ is constant for groups of nuclei, whilst $k$ varies from location to location in the sample, with the total distribution of $k$ values being Gaussian with a central value $k_o$, and width of the distribution $w$, whilst $k$ is supposed to not vary with time. It is assumed that impingement in each location can be approximated by the JMAK expression. In Fig. 1 several curves for various values of $w/k_o$ are presented (in all cases $n = 1\frac{1}{2}$, i.e. parabolic growth with $N_{dim} = 3$ is considered). Equation 3 can represent all curves in Fig. 1 very well (accuracy better than 2% up to $\alpha = 0.9$). In Fig. 2 the values of $\eta_i$ obtained from an optimised fit as in Fig. 1 are presented as a function of the width of the Gaussian $k$ distribution. Note that when the distribution broadens $\eta_i$ approaches 1 whilst for an infinitely narrow distribution the JMAK equation is obtained and $\eta_i = \infty$.

## 2.3. Growth rates that vary with position and time: vacancy loss to defects

To consider a more specific example of a process in which growth rates vary with position and time, the average transformation for a reaction that is influenced by annihilation of vacancies is calculated. The following hypothetical situation, which is on many points inspired by processes occurring during precipitation, is considered. An alloy is quenched from high temperature to a lower ageing temperature. At the ageing temperature excess vacancies diffuse to lattice defects (grain boundaries, dislocations, etc.), where they annihilate. Simultaneously, a transformation (for instance precipitation of alloying elements) occurs, for which the rate is dependent on the amount of vacancies. We will consider the case of site saturation only, i.e. we will assume all nuclei to be formed in the very early stages of the transformation and, effectively, transformation occurs with a constant number of nuclei. (This is a valid approximation for many precipitation reactions in Al based alloys, see e.g. [7,22,24].) For this example we will assume that only annihilation at grain boundaries is relevant, and to limit computations we will assume grains to be thin in one direction, i.e. vacancy diffusion occurs effectively in one single direction. The solution to this diffusion problem is known (see e.g. [45]); the vacancy concentration, $x_v$, as a function of the distance from the centre of the grain, $y$, is given by:

$$x_v(y,t) = x_v(y,0)\left[1 - \sum_{n=1}^{\infty}(-1)^n\left(erfc\frac{(2n+1)d - y}{2\sqrt{Dt}} + erfc\frac{(2n+1)d + y}{2\sqrt{Dt}}\right)\right] \quad (5)$$

where $d$ is the half-thickness of the grain, $x_v(y,0)$ is the initial concentration of vacancies, which is assumed to be homogeneous. The rate constant $k$ (from Equation 1) is assumed to be a linear function of the concentration of vacancies, $x_v(y,t)$, where $y$ is the distance from the centre of the grain, i.e.:

$$k(y,t) = k_1 + (k_2 - k_1)(x_v(y,t)/x_v(t=0)) \quad (6)$$

where $k_1$ is the rate constant in material unaffected by annihilation at grain boundaries, and $k_2$ is the rate constant in material in which the vacancy concentration has reached the equilibrium value. The assumed linear relationship between $k$ and $x_v$ is based on the notion that the frequency of an alloying atom making a diffusional 'jump' from one lattice position to a next is

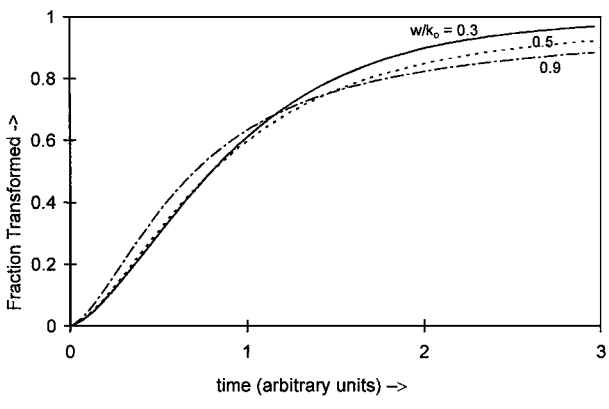


*Figure 1* Averaged fraction transformed for normally (Gaussian) distributed JMAK processes, with $w/k_o = 0.3$, 0.5 and 0.9, $n = 1.5$.

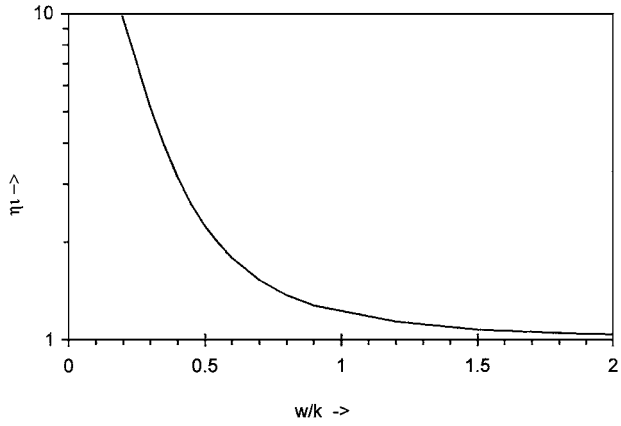


*Figure 2* Value of $\eta_i$ for an optimal fit of Equation 3 to averaged fraction transformed for normally (Gaussian) distributed JMAK processes, $n = 1.5$ (Fit is optimised for $\alpha$ between 0 and 0.8).

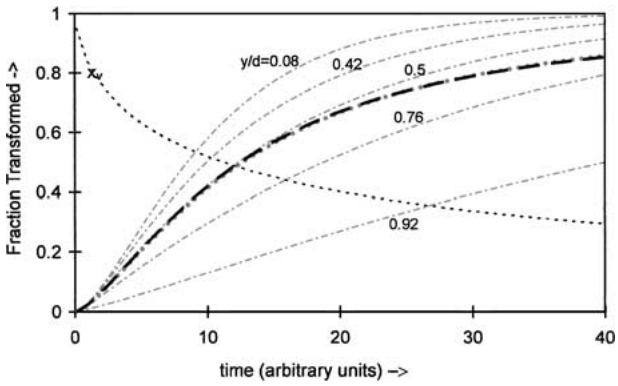


*Figure 3* Transformation curves for a reaction which is influenced by vacancy annihilation ($k_2/k_1 = 7$). Presented are fractions transformed at various positions in the sample (———), the average fraction transformed (• • • •) and a fit of the latter based on Equation 3 with $\eta_i = 1.15$ and $n_S = 1.42$ (— —). Also presented is the average concentration of vacancies remaining in the sample (· · · ·).

mainly dependent on the amount of unoccupied lattice sites. It is assumed that all regions of the sample transform according to JMAK kinetics (Equation 1) with variable $k(y, t)$ as given above and a constant reaction exponent $n$.

In order to evaluate a realistic example we will consider precipitation in Al based alloys. Lattice parameter determinations of liquid quenched Al-Si and Al-Mg alloys aged at about 150°C indicate that free vacancies are annihilated before significant precipitation occurs [46]. Hence, these vacancies will have no influence on precipitation, and only vacancies bound to alloying atoms will influence precipitation. As diffusion of these vacancies is slowed down by binding to the alloying atoms, their annihilation will generally overlap with the precipitation process. Results of the evaluation of the above equations are presented in Fig. 3. For the calculations, realistic $D$, $k_1$ and $k_2$ values are used: $k_2/k_1$ is taken as 7 (see Appendix I), whilst $D$ is adjusted such that the average vacancy concentration is halved when $\alpha = 0.5$. Again the overall transformation curve has been fitted with Equation 3. Also for this case the JMAK equation (Equation 1) can not describe the overall transformation, whilst Equation 3 provides a very accurate representation of the overall kinetics. By variation of the parameters ($k_1$, $k_2$, $D$, $d$, $n_S$) it was verified that the latter conclusion is generally valid, provided $k_2/k_1$ is smaller than about 20. It is interesting to note that the optimal $n_S$ for fits in Fig. 3 is somewhat lower than the $n_A$ in the JMAK equation. This is due to the decrease of the vacancy concentration with time, which has a decelerating effect on the transformation.

Obviously, several assumptions made in the presented example are specific to the type of reaction, geometries of defects or grains and the rate of vacancy annihilation. Nevertheless, several generally valid conclusions, which have been verified by varying parameters, can be drawn from this model. Firstly, vacancy loss changes the kinetics of the reaction: Equation 1 is not valid and instead Equation 3 can give a good description of the kinetics. The deviation from Equation 1 is due to two effects: i) in the vacancy diffusion zone $k$ values vary with position leading to a "smearing out" of the transformation curve similar to the process described in Section 2.2, and ii) due to the annihilation of vacancies the effective value of $k$ decreases with time, leading to a deceleration as compared to JMAK kinetics. Further, the overall average transformation curve depends on $k_1$, $k_2$, $D$ and $d$.

## 2.4. Interfacial energy: the Gibbs-Thomson effect

Due to a contribution of surface energy, the Gibbs free energy (per mole) of a multi-phase sample will depend on the interfacial area, i.e. on the size of the phases. If the product of a reaction consists of at least two phases this interfacial energy contribution will influence the local metastable equilibrium state. In precipitation reactions this is known as the Gibbs-Thomson (or capillarity) effect (see e.g. [47]): the local metastable solubility of alloying elements around a precipitate increases with decreasing radius of that precipitate (i.e. increasing local curvature of the interface). In the following it will be shown that for precipitation reactions this effect has to be taken into account and that the Gibbs-Thomson effect significantly modifies the overall kinetics of a precipitation reaction.

Consider a precipitation reaction in which precipitates are spherical, with radius $r$. At the start of the transformation, $N_p$ nuclei are present, and during the transformation nucleation is negligible. The precipitate/matrix interfacial energy, $\sigma_s$, is constant, whilst the equilibrium solubility is taken according to a regular solution model (see e.g. [48]):

$$c_{\mathrm{eq}}(T) = c_\infty \exp\left(\frac{-\Delta H_{\mathrm{sol}}}{k_B T}\right) \tag{7}$$

where $c_\infty$ is a constant and $\Delta H_{\mathrm{sol}}$ is the enthalpy of formation (in J per mole precipitate). In keeping with this model it is assumed that the metastable solubility, $c_{\mathrm{ms}}$, is determined by an effective enthalpy of formation of precipitates, $\Delta H_{\mathrm{eff}}$, which takes the energy of the interface into account:

$$c_{\mathrm{ms}}(T) = c_\infty \exp\left(\frac{-\Delta H_{\mathrm{eff}}}{k_B T}\right) \tag{8}$$

$$\Delta H_{\mathrm{eff}} = \Delta H_{\mathrm{sol}} + Q(r, \sigma_s) \tag{9}$$

where $\mathrm{Q}(r, \sigma_s)$ is the total energy related to the interface per mole precipitate, which can be calculated straightforward to yield:

$$\Delta H_{\mathrm{eff}} = \Delta H_{\mathrm{sol}} - \frac{N_p \sigma_s}{c_o \rho_a} B_1 \left(\frac{c_o \rho_a}{N_p \rho_p}\right)^{2/3} \xi^{-1/3} \tag{10}$$

where $\rho_a$, $\rho_p$ are the densities if the matrix phase and the precipitate, respectively, $c_o$ is the initial concentration of solute in the matrix, $B_1 = 4\pi/(4/3\pi)^{2/3}$, $\xi$ is the fraction of the initial solute present that has precipitated. One key point follows directly from this description: if

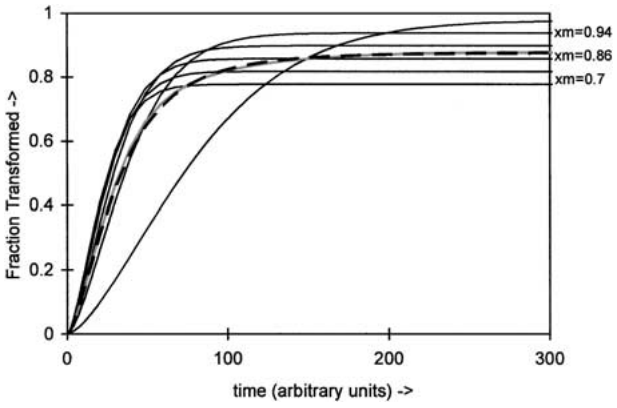


*Figure 4* Transformation curves for a reaction which is influenced by the Gibbs-Thomson effect. Presented are curves for various values of $x_m$.

no coarsening occurs, the amount of solute that can precipitate depends on $r$, and the latter, in turn, depends on the amount of growing nuclei. This maximum amount of solute that can precipitate is given by:

$$\xi_m = 1 - \frac{c_{\mathrm{ms}}}{c_{\mathrm{o}}} \tag{11}$$

and from Equations 8 and 9 with $\xi = \xi_m$, $\xi_m$ can be evaluated numerically.

In a simplified assessment of the influence of capillarity of transformation rates, we will calculate transformation curves for various values of $N_p$, assuming that the amount of precipitates during the transformation is constant. The transformation for each value of $N_p$ is assumed to follow JMAK kinetics, i.e.:

$$\frac{\xi}{\xi_m} = 1 - \exp(-[kt]^{n_A}) \tag{12}$$

In this equation $k^n$ is proportional to $N_p$. For the various parameters we will take values for precipitation of Si from Al, the interfacial energy in this system has been estimated at 1.5 J/m$^2$ [48]. Results, presented in Fig. 4, illustrate the main effects of the interfacial energy. For high $N_p$ the initial transformation rate is high, but as $\xi_m$ is low the sample will not attain equilibrium without coarsening. For lower $N_p$ the initial transformation rate is lower, but as $\xi_m$ is closer to equilibrium, the transformation rate for the later stages will be higher. Whilst Fig. 4 illustrates some of the issues at play, it is clear that an exact model would have to take into account the size-dependent metastable solubility around each growing particle as well as a continuous evolution from growth to coarsening, but no such models are available.‡ To obtain an estimate of the magnitude of the deviation from JMAK kinetics two rather crude estimates for such a model were analysed. In a first attempt, evolution from growth to coarsening was approximated by taking the average of the processes in Fig. 4, results are indicated by the grey line in Fig. 4. It is interesting to note that this averaged process can be represented very well with Equation 3 (dotted line in Fig. 4, for which $\eta_i = 2.5$). In a slightly more refined treatment of the continuous evolution from growth to coarsening was obtained from a simplified form of the LSW theory (see Appendix II). Again the process can be represented very well with Equation 3.

The above example shows that for precipitation in Al-Si, the Gibbs-Thomson effect causes a modification of the overall kinetics of the reaction. The processes in this example are generally applicable to any reaction that results in the creation of a new interface.

## 2.5. Internal stresses

If either nucleation rates or growth rates are sensitive to stresses, internal stresses in a sample can influence the reaction kinetics. These stresses will vary according to position in the sample and as a result the overall transformation will be the average of processes with different nucleation rates or growth rates. In Section 2.2 it was shown that this leads to a smearing out of the transformation curve and that JMAK kinetics is no longer valid. If the distribution of the different nucleation rates or growth rates is Gaussian or in approximation Gaussian, Equation 3 will yield a good description of the overall reaction.

An especially striking example of the effect of internal stresses on reactions can be found in heat treatable Al-based MMCs, where the stresses around reinforcing ceramic particles cause precipitation rates to vary with distance from the reinforcing particle and on orientation of the precipitate relative to the stress field [50, 51]. In monolithic alloys internal stresses will be much lower and effects correspondingly smaller. However, as elastic properties are generally anisotropic, temperature changes will inevitably create internal stresses in all polycrystalline samples. Thus internal stresses can be expected in all types of samples and for reactions which are sensitive to those stresses, deviations from JMAK reactions can be anticipated.

## 2.6. Transformations with anisotropic growth rates

In transformations producing particles with anisotropic growth rates, i.e. where particles are not equiaxed, fast moving interfaces can impinge on slow moving interfaces. This can mean that areas that could be transformed by the fast moving interface if it had not been stopped, are effectively 'shielded' by the blocking particle. This mechanism is depicted schematically in Fig. 5. (The particular example depicts a transformation in which the preferential growth directions are oriented normal to each other. This blocking mechanism will cause impingement to be stronger as compared to JMAK type impingement. As this impingement is only important after growing transformed regions reach a certain minimum size, this type of deviation from the JMAK assumptions will influence only the later stages of the reaction where it will cause an additional reduction of the reaction rate. This type of deviation from

‡ An approximate model incorporating assumptions concerning the continuous evolution from growth to coarsening stage has recently been presented by Deschamps and Brechet [49].

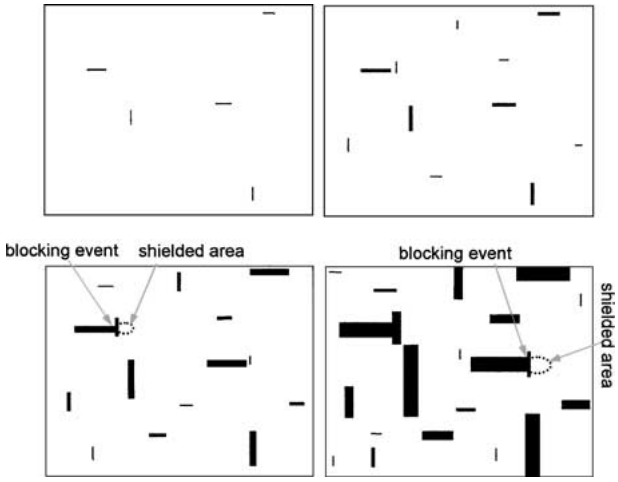


*Figure 5* Schematic illustration of blocking during the growth of anisotropic particles. The figure depicts a 2D transformation with nucleation and growth in which the growing particles are oriented normal to each other.

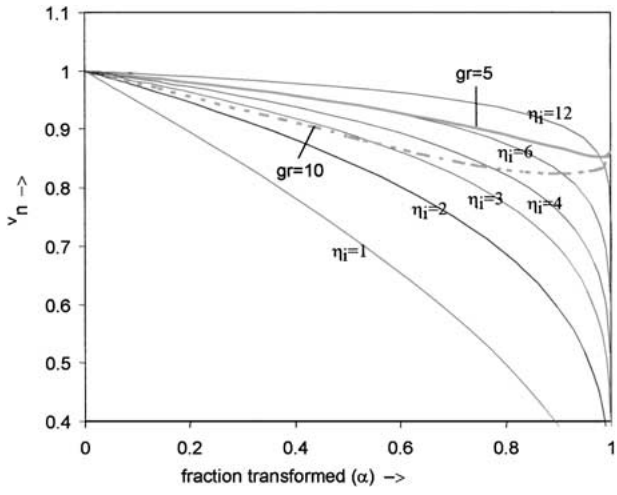


*Figure 6* Avrami exponents vs. fraction transformed for $\eta_i = 1$ to 12, as calculated from Equation 3. Also presented are Avrami exponents for a one dimensional model representing the case of blocking resulting from anisotropic growth with growth rate anisotropy $g_r = 5$ and 10 (data from Ref. 37). Note that for a large range of $\alpha$ values the latter data can be fitted well by Avrami exponents from Equation 3.

JMAK kinetics for the case of linear growth has been modelled by Birnie and Weinberg [34–37] and below it will be shown that also for these types of deviations from the JMAK assumptions Equation 3 will give a good approximation of the overall reaction kinetics.

In Fig. 6 the Avrami exponent as calculated from Equation 3 is plotted vs. $\alpha$, where they are compared with results obtained by Birnie and Weinberg [34] for a 1D model of particles growing with anisotropic growth rates. These curves resemble each other providing $\alpha$ is limited to about 0.9 and growth rate anisotropies are smaller than 10. Hence for these growth rate anisotropies Equation 3 will give a good representation of the overall transformation, with $\eta_i$ increasing with growth rate anisotropy. For higher growth rate anisotropies Weinberg and Birnie's results tend to deviate from Equation 3, especially for high $\alpha$. It should be noted that the case of a 1D model with random orientations of the elongated precipitates, as discussed here, represents a specific case, and true quantitative analysis of impingement in more realistic cases requires more complicated models.

### 2.7. Impingement on defects, inclusions and interfaces

Impingement on defects, inclusions, interfaces, and generally all obstacles other than neighbouring transformed areas will influence the overall kinetics of a reaction. As this impingement is only important after growing transformed regions reach a certain minimum size, this type of deviation from the JMAK assumptions will influence only the latter type of the reaction where it will cause a deceleration. Impingement against defects, like grain boundaries and inclusions has been investigated in some detail by other researchers [30–32, 40]. Within the context of this paper it is especially interesting to note that Tagami and Tanaka approached the problem of restricted nucleation and growth within a thin plate (especially the example of a Si layer bounde by $SiO_x$ was used) by making the approximation that transformation occurs by the instantaneous transformation of domains all of which reach an identical, fixed size in the extended volume. It was shown that in this case Equation 3 is reproduced. Hence, whilst in previous cases discussed it could be shown that Equation 3, yields a good approximation of the transformation kinetics, in this simplified treatment of impingement on planar obstacles Equation 3 exactly reproduces the kinetics.

## 3. The relation between the breakdown of JMAK assumptions and the overall impingement coefficient $\eta_i$

In the previous section we have investigated the effects that result from the breakdown of the preconditions for the single JMAK process (Equation 1). Generally, single microstructural or thermodynamic phenomena result in one or more of these preconditions being violated, but it is possible to separate out the different effects and assign them to four main classes of deviations. The first one we will refer to as 'inhomogeneity type' deviations: $k$ and $n$ are constant over the whole of the sample, but the maximum amount that can transform is position dependent. In Section 2.1 it was shown that a pure 'inhomogeneity type' deviation of the JMAK assumptions does not affect the overall type of kinetics: if individual areas transform according to JMAK kinetics the overall average reaction does so too. The second type we will refer to as 'rate distribution type' deviations: $n$ and the maximum amount that can transform are constant, but $k$ is position dependent. In Section 2.2 it was shown that a pure 'rate distribution type' deviation affects the overall type of kinetics: JMAK kinetics is no longer valid and, providing the distribution of the different nucleation rates or growth rates is in approximation Gaussian, Equation 3 yields a good description of the overall reaction, with $n_S \cong n_A$. It was shown that the Gibbs-Thomson effect leads to a breakdown of the JMAK assumptions as a result of

this rate distribution type breakdown intermixed with an 'inhomogeneity type' effect. The third group of deviations will be referred to as 'blocking' type deviations: growth is blocked in a way that is not taken into account in the JMAK equation. Examples are blocking by defects, grain boundaries, edges of a sample or inert particles, and also blocking due to anisotropic growth rates of particles is considered to be part of this group. The fourth type of deviation from the assumptions for JMAK kinetics is time dependency of $k$. This 'time-dependent rate type' deviation was encountered mixed with 'rate distribution type' deviations in the example concerning vacancy diffusion and annihilation. Also in this case Equation 3 provided a good approximation of the overall kinetics, but $n_S$ is no longer equal to $n_A$.

From the above it is concluded that if kinetics are altered due to a deviation from the JMAK assumptions, the resulting kinetics of the overall transformation can generally be well described by Equation 3. This indicates that for each individual type of breakdown of JMAK assumptions Equation 3 will, in good approximation, describe the transformation. A subsequent step in the analysis will be to analyse the effect that a superposition of different mechanisms (Gibbs-Thomson effect, vacancy annihilation, etc.) will have on the kinetics of the reaction. To perform such an analysis one may attempt to construct a microstructural model for a reaction in which for instance the Gibbs-Thomson effect and vacancy diffusion and annihilation are taken into account simultaneously. However, such a complicated analysis can be avoided and a generally valid approximate solution for this superposition can be found in the following way. Analyse for each different mechanism the resulting kinetics of the transformation separately, and fit Equation 3 to it. From Fig. 2 one can derive which distribution of $k$ values with width $w$ is equivalent with this. Hence for each mechanism, $j$, one finds a $w_i$. Then, superposition of Gaussian distributions leads to:

$$w_t^2 = \sum_j w_j^2 \tag{13}$$

Once $w_t$ is obtained, one can subsequently obtain the appropriate $\eta_i$ for the overall reaction which accounts for all mechanisms which cause a breakdown of the JMAK assumptions.

## 4. Application of the kinetic equation

For the purpose of the present paper, data on a number of reactions have been considered: isothermal calorimetry data on precipitation of $\beta'$ at 180°C on an air-cooled Al-16at%Mg alloy, isothermal calorimetry data precipitation of the $L1_2$ ordered phase in air-cooled Al-16at%Mg at 80 and 85°C, precipitation of the $L1_2$ ordered phase in water quenched Al-Li and isothermal calorimetry data on precipitation of the Si phase in an air cooled Al-6at%Si alloy (for experimental details see [52]). In line with previous publications [21–27] this new data could be fitted well by Equation 3, with $\eta_i$ close to unity, whilst Equation 1 fitted badly. At present a detailed analysis of this new data will be limited to the data on the Al-Si alloy.

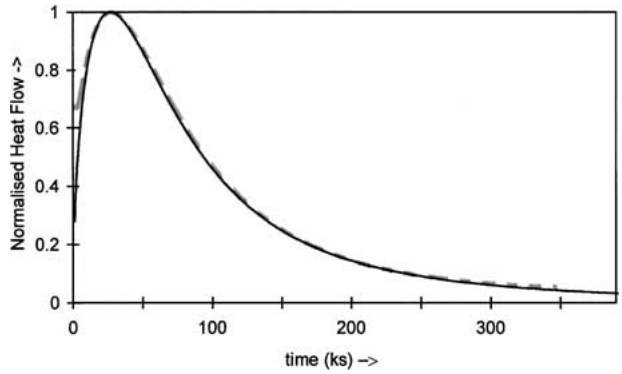


*Figure 7* Normalised heat flow curve for precipitation in air-cooled Al-6at%Si at 230°C (dashed grey line). The fit (thin, black line) is obtained with Equation 3 and $\eta_i = 1.1$, $n_S = 1.5$.

In Fig. 7 a typical example of an isothermal calorimetry curve for an air-cooled Al-6at%Si alloy is presented. Differential Scanning Calorimetry (DSC) experiments have indicated that for Al-Si alloys cooled at these relatively low rates no significant nucleation occurs during the course of the reaction [21, 24], and hence $n_S$ should equal 1.5 (see Equation 2). For this reaction several JMAK assumptions are thought to fail, most notably because of the Gibbs-Thomson effect, and because of vacancy annihilation in the course of the precipitation reaction. The heat flow is proportional to the rate of the reaction and hence the normalised calorimetry curve is fitted by $d\alpha/dt$ obtained from Equation 3. Fig. 7 shows that a near perfect fit of theory and experiment is obtained for $\eta_i = 1.1, n_S = 1.5$. (Only for $t < 10$ ks, i.e. in the very first stages of the reaction, some deviation between theory and experiment occurs. This is due to a separate precipitation process via growth of undissolved Si particles as indicated in earlier studies [21, 24]) The value $n_S = 1.5$ obtained from the fit corresponds to diffusion controlled growth of pre-existing nuclei, whilst the obtained value of $\eta_i$ can be explained in the following way. The studied examples in Sections 2.3 indicate that the Gibbs-Thomson effect results in $\eta_i = 2.5$. The corresponding width of a Gaussian distribution can be obtained with Fig. 2 and this results in $w_1 = 0.47$. The calculations in Section 2.4 indicated that for vacancy annihilation in an Al-based alloy $\eta_i \approx 1.15$, i.e. with Fig. 2: $w_2 = 1.13$. With Equation 12 it follows that for the overall reaction $w_t = 1.2$ and $\eta_i = 1.14$. The latter value is very close to the one obtained in Fig. 7, indicating that the present analysis of the deviation from JMAK kinetics is sound.

Generally, the activation energy for diffusion of vacancies and for diffusion of alloying atoms will be different. This implies that the relative rates of vacancy annihilation and of precipitation will be temperature dependent and as a result of this $\eta_i$ will be temperature dependent. In line with this it has been noted in previous works [21, 24] that for DSC experiments where Si precipitates at about 350–400°C, $\eta_i$ is about 2.2, i.e. significantly larger than for isothermal precipitation at 230°C. This finding can be explained semi-quantitatively on the basis of the model presented in Section 2.3. For this we

first calculate the relative vacancy annihilation and precipitation rates at 400°C using the activation energies for diffusion of vacancies and for diffusion of alloying atoms in Al-Si (about 0.66 and 0.95 eV, respectively). The precipitation curve obtained via this procedure can be fitted well with Equation 3 with $\eta_i = 2.9$ (curve not presented), which explains the difference in $\eta_i$ for the two experiments.

## 5. Concluding remarks

In the previous section as well as in previous publications [21–27] experimental data on a large number of mostly diffusion controlled reactions have been studied; all could be fitted well by Equation 3, with $\eta_i$ close to unity. Hence, it must be concluded that for precipitation reactions the preconditions for the single JMAK process (Equation 1) are generally not fulfilled. The theory and examples presented in Section 2 give a theoretical explanation for this finding as it was shown that, in good approximation, deviations from the JMAK assumptions, and the superpositions of several of these deviations occurring for a single reaction, all lead to the kinetic equation Equation 3. For precipitation in an air-cooled Al-Si alloy (see previous section), the single most important mechanism resulting in deviations from the JMAK assumptions appears to be annihilation of vacancies. Further also the Gibbs-Thomson effect played a role.

Based on the findings in this paper it is recommended that in any analysis of transformation curves it be taken into account that transformation curves can deviate from JMAK kinetics due to a wide variety of reasons. Equation 3, which can take account (at least in good approximation) of the wide range of deviations considered in Section 3 of the present paper, can be used very effectively to this end.

## 6. Conclusions

The JMAK kinetic equation is valid only under a number of preconditions: product phases are randomly distributed, nucleation is random, growth rates are constant and independent of position in the sample, impingement against objects other than neighbouring domains of the product phase is negligible, growth is isotropic, and the equilibrium state is constant. Several mechanisms which cause deviations from these preconditions have been identified, they include: the Gibbs-Thomson (or capillary) effect, vacancy annihilation, blocking due to anisotropic growth, internal stresses and impingement on defects. These deviations lead to different modifications of the overall transformation, which can all be approximated well by a single equation (Equation 3). Also the kinetics resulting from superpositions of the different modifications can be described well by the above equation. The validity of the equation is assessed by comparison with transformation curves obtained for precipitation in an Al-Si alloy. A very good correspondence between experiment and model is found and the value for $\eta_i$ obtained from the fit could be explained quantitatively in terms of two mechanisms leading to deviations from the JMAK assumptions: the Gibbs-Thomson effect and vacancy loss.

## Appendix I

In a dilute alloy with low concentrations of vacancies (i.e. di-vacancies can be neglected), vacancies are present as free vacancies, and vacancies bound by solute elements $s_i$. The total concentration of vacancies, $C'_v$ in an FCC metal can be estimated as [53]:

$$C'_v = C_v \left\{ 1 - 12 \sum_{1}^{n=i} C_i + 12 \sum_{1}^{n=i} C_i \exp\left( \frac{E^b_{s_i - v}}{k_B T} \right) \right\} \tag{14}$$

where $C_v$ is the concentration of vacancies in the pure metal, $E^b_{s_i - v}$ is the binding energy of element $s_i$ with a vacancy, and $C_i$ is the concentration of solute $i$. From this the amount of vacancies bound by atoms of a certain a type can be estimated.

If artificial ageing is performed on alloys which are solution treated at different temperatures, first the free vacancies are annihilated, and one generally finds that precipitation rates increases with solution treatment temperature, $T_s$. This is ascribed to enhanced diffusion resulting from increased amounts of vacancies bound to solute atoms. By comparing precipitation rates of an alloy quenched from different solution treatment temperatures it is possible to estimate the effect of vacancies on the ratio $k_2/k_1$. Such an estimate is obtained for an Al-Mg and an Al-Si alloy.

DSC experiments at heating rate 20 °C/min on an Al-13at%Mg alloy solution treated at 420 and 470°C showed that the precipitation occurs around 350°C and that in the alloy solution treated at the lower temperature precipitation was retarded by about 18°C [54]. Using Equation A3 in Ref. [55] in combination with the activation energy for precipitation (about 0.9 eV) this can be converted to a difference in isothermal precipitation rate. Then, with Equation 14 in combination with the binding energy of solute atom and vacancy (estimated at about 0.36 eV for Mg), the ratio $k_2/k_1$ can be obtained. For the experiments on Al-13at%Mg this results in $k_2/k_1 = 6$, and the latter value is independent of precipitation temperature.

Precipitation in a liquid-quenched (LQ) Al-1.3at%Si alloy is slower as compared to the water-quenched Al-1.3at%Si alloy. This is interpreted to be due to a lower vacancy concentration in the LQ alloy resulting from lower quenching rate for temperatures below the solidus [46], and similarly to the method presented above, a calculation of the ratio $k_2/k_1$ can be performed for the Al-1.3at%Si alloy. No data is available on the effective solution treatment temperature, $T_{\text{eff}}$, which corresponds to the vacancy concentration in the LQ alloy. It is estimated to be about 100°C below the solidus (i.e. at about 490°C), whilst the solute-vacancy binding energy is taken as 0.15 eV. This results in $k_2/k_1 = 8$. A reduction of $T_{\text{eff}}$ by about 50°C results in $k_2/k_1 = 5$.

In conclusion of this appendix it is estimated that for precipitation in Al-based alloys $k_2/k_1$ is generally in the order of 5 to 8.

## Appendix II

To derive a simplified treatment of continuous evolution from growth to coarsening we will proceed as follows. According to the classical LSW coarsening theory (see e.g. [56] and references therein) is applied:

$$\bar{r}^3 - \bar{r}_o^3 = k_{\mathrm{co}} t \tag{15}$$

where $\bar{r}$ is the average radius of the precipitates, $\bar{r}_o$ is the average initial radius of the precipitates and $k_{\mathrm{co}}$ is the rate constant for coarsening. By assuming that $\bar{r}_o \ll \bar{r}$ and using that $1/N_p$ is proportional to $\bar{r}^3$ it is derived:

$$\frac{\mathrm{d}(1/N_p)}{\mathrm{d}t} = k_N \tag{16}$$

where $k_N$ is a constant. It thus follows:

$$N_p = \left( k_N t + \frac{1}{N_o} \right)^{-1} \tag{17}$$

Using the latter two equations together with Equations 7–11 yields transformations functions for given $c_o$, $\sigma_s$, $N_{\mathrm{o}}$ and $k$. A range of combinations of these parameters was investigated, and in all cases the transformation could be fitted well with Equation 3.


## Acknowledgements

Dr A.-M. Zahra of the Centre de Thermodynamique et de Microcalorimétrie du CNRS, Marseille, France, is gratefully acknowledged for providing isothermal calorimetry data and for critically reading drafts of the manuscript.


## References


1. J. W. CHRISTIAN, "The Theory of Transformation in Metals and Alloys," 2nd ed., Part 1. (Pergamon Press, Oxford, UK, 1975).
2. F. L. CUMBRERA and F. SANCHEZ-BAJO, *Thermochim. Acta* **266** (1995) 315.
3. V. SESSA, M. FANFONI and M. TOMELLINI, *Phys. Rev. B.* **54** (1996) 836.
4. M. TOMELLINI and M. FANFONI, *ibid.* **55** (1997) 14071.
5. C. DEW. VAN SICLEN, *ibid.* **54** (1996) 11845.
6. C. MICHAELSEN, M. DAHMS and M. PUFF, *ibid.* **53** (1996) 11877.
7. M. J. STARINK, *J. Mater. Sci.* **32** (1997) 4061.
8. D. H. BRATLAND, O. GRONG, H. SHERCLIFF, O. R. MYHR and S. TJOTTA, *Acta Mater.* **45** (1997) 1.
9. A. BORREGO and G. GONZALEZDONCEL, *Mater. Sci. Eng. A* **245** (1998) 10.
10. *Idem., ibid.* **252** (1998) 149.
11. M. I. LUPPO and J. OVEJEROGARCIA, *Mater. Characterisation* **40** (1998) 189.
12. I. SHIMIZU, *Phil. Mag. A* **79** (1999) 1217.
13. R. A. RAMOS, P. A RIKVOLD and M. A. NOVOTNY, *Phys. Rev. B* **59** (1999) 9053.
14. O. M. BECKER, *J. Chem. Phys* **96** (1992) 5488.
15. EON-SIK LEE and YOUNG G. KIM, *Acta Metall. Mater.* **38** (1990) 1669.
16. V. ERUKHIMOVITCH and J. BARAM, *Phys. Rev. B* **50** (1994) 5854.
17. *Idem., ibid.* **51** (1995) 6221.
18. J. B. AUSTIN and R. L. RICKETT, *Trans. Am. Inst. Min. Engrs.* **135** (1939) 396.
19. R. A. VANDERMEER and P. GORDON, in "Recovery and Recrystallization in Metals," edited by L. Himmel (Gordon and Breach Science Publishers, New York, NY, 1963) p. 211.
20. L. Q. XING, J. ECKERT, W. LOSER, L. SCHULTZ and D. M. HERLACH, *Phil. Mag. A* **79** (1999) 1095.
21. M. J. STARINK and A.-M. ZAHRA, *Thermochim. Acta* **292** (1997) 159.
22. *Idem., J. Mater. Sci. Lett.* **16** (1997) 1613.
23. *Idem., Acta Mater.* **46** (1998) 3381.
24. *Idem., Phil. Mag. A* **77** (1998) 187.
25. M. J. STARINK, C. Y. ZAHRA and A.-M. ZAHRA, *J. Therm. Anal. Calorim.* **51** (1998) 933.
26. M. J. STARINK, P. WANG, I. SINCLAIR and P. J. GREGSON, *Acta Mater.* **47** (1999) 3841.
27. M. K. MILLER, K. F. RUSSELL, P. J. PAREIGE, M. J. STARINK and R. C. THOMSON, *Mater. Sci. Eng. A* **250** (1998) 49.
28. J. F. NIE and B. C. MUDDLE, *J. Phase Eq.* **19** (1998) 543.
29. M. HILLERT, *Acta Metall* **7** (1959) 653.
30. T. TAGAMI and S. TANAKA, *Acta Mater.* **45** (1997) 3341.
31. *Idem., ibid.* **46** (1998) 1055.
32. *Idem., J. Mater. Sci.* **34** (1999) 355.
33. GE YU and J. K. L. LAI, *J. Appl. Phys.* **79** (1996) 3504.
34. D. P. BIRNIE III and M. C. WEINBERG, *J. Chem. Phys.* **103** (1995) 3742.
35. M. C. WEINBERG and D. P. BIRNIE III, *ibid.* **105** (1996) 5139.
36. D. P. BIRNIE III and M. C. WEINBERG, *Physica A* **230** (1996) 484.
37. M. C. WEINBERG and D. P. BIRNIE III, *J. Non-Cryst. Solids* **202** (1996) 290.
38. P. UEBELE and H. HERMANN, *Modell. Simul. Mater. Sci. Eng.* **4** (1996) 203.
39. N. X. SUN, X. D. LIU and K. LU, *Scr. Mater.* **34** (1996) 1201.
40. C. F. PEZZEE and D. C. DUNAND, *Acta Metall. Mater.* **42** (1994) 1509.
41. T. PUSZTAI and L. GRANASY, *Phys. Rev. B* **57** (1998) 14110.
42. F. S. HAM, *J. Appl. Phys.* **30** (1959) 1518.
43. *Idem., Quarterly Appl. Math.* **17** (1959) 137.
44. E. PINEDA and D. CRESPO, *Phys. Rev. B* **60** (1999) 3104.
45. H. S. CARSLAW and J. C. JAEGER, in "Conduction of Heat in Solids," 2nd ed. (Clarendon Press, Oxford, UK, 1959).
46. P. VAN MOURIK, Ph.D. thesis, Delft University of Technology (Delft University Press, Delft, The Netherlands, 1988).
47. N. KULKARNI and N. DEHOFF, *Acta Mater.* **45** (1997) 4963.
48. M. VAN ROOYEN and E. J. MITTEMEIJER, *Metall. Trans. A* **20** (1989) 1207.
49. A. DESCHAMPS and Y. BRECHET, *Acta Metall.* **47** (1999) 293.
50. P. B. PRANGNELL and W. B. STOBBS, in Proc. 12th RISO International Symposium: MMCs- Processing, Microstructure and Properties, Roskilde, Denmark, Sept. 1991 (RISO, Roskilde, Denmark, 1991) p. 603.
51. P. B. PRANGNELL, T. DOWNES, W. B. STOBBS and P. J. WHITHERS, *Acta Metall. Mater.* **42** (1994) 3425.
52. M. J. STARINK and A.-M. ZAHRA, *Mater. Sci. Forum* **217-222** (1996) 795.
53. S. ÖZBILEN and H. M. FLOWER, *Acta Metall. Mater.* **37** (1989) 2993.
54. M. J. STARINK and A.-M. ZAHRA, unpublished research, 1997.
55. M. J. STARINK and P. J. GREGSON, *Mater. Sci. Eng. A* **211** (1996) 54.
56. R. PODURI and L.-Q. CHEN, *Acta Mater.* **46** (1998) 3915.



*Received 25 July 2000*
*and accepted 21 February 2001*